Available online at www.sciencedirect.com

ScienceDirect

Mendeleev Commun., 2023, **33**, 823–825

Mendeleev Communications

Structure and antiradical activity of *N*-monosubstituted amino acid derivatives of fullerene C_{60} in aqueous colloidal solutions

Mikhail V. Voronkov,[a] Vladimir A. Volkov,*[a] Vladimir V. Volkov,[b] Valentina S. Romanova,[c] Irina G. Plashchina[a] and Egor V. Sidorsky[c]

[a] *N. M. Emanuel Institute of Biochemical Physics, Russian Academy of Sciences, 119334 Moscow, Russian Federation. E-mail: vl.volkov@mail.ru*
[b] *A. V. Shubnikov Institute of Crystallography, FSRC 'Crystallography and Photonics', Russian Academy of Sciences, 119333 Moscow, Russian Federation*
[c] *A. N. Nesmeyanov Institute of Organoelement Compounds, Russian Academy of Sciences, 119334 Moscow, Russian Federation*

DOI: 10.1016/j.mencom.2023.10.028

The dimensional characteristics of nanoparticles of *N*-monosubstituted amino acid derivatives of fullerene C_{60} (AAFDs) in aqueous colloidal solutions, determined by dynamic light scattering (DLS) and small-angle X-ray scattering (SAXS), were compared. The DLS data on the dimensional characteristics of fullerene C_{60} and AAFD nanoparticles, obtained at scattering angles of 90° and 173°, are close in values with a correlation coefficient of 0.89, and the SAXS data indicate that AAFDs form ordered structures in solution. Based on the results of DLS and the ability of fullerene and AAFDs to inhibit peroxyl radicals, it can be concluded that varying the concentrations of the studied compounds in the range from 10^{-7} to 10^{-3} M does not affect the degree of aggregation of their nanoparticles.

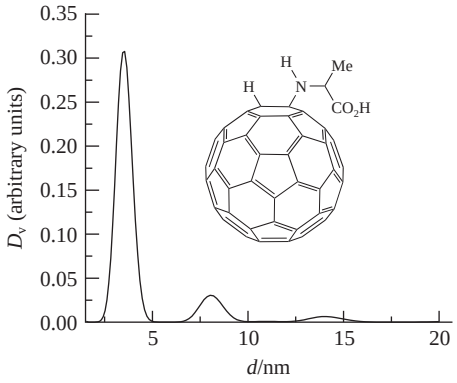

Keywords: fullerene C_{60}, nanoparticles, dynamic light scattering, small-angle X-ray scattering, antiradical activity, ORAC, fluorescence, oxidation, liposomes.

Dedicated to Academician M. P. Egorov on the occasion of his 70th birthday anniversary with wishes of good health and new successes in the development of Russian chemical science.

The insolubility of fullerenes in water creates some obstacles for their use to influence processes in biological systems. One effective way to solubilize these objects is to attach a water-soluble substituent to the fullerene, which increases the solubility in water while retaining other properties inherent to fullerenes. Solubilized forms of fullerenes, in particular amino acid derivatives, exhibit various biological activities, including antioxidant, antiviral, antibacterial, antitumor, neuroprotective and others.[1–5] It should be noted that the solubilized forms of fullerenes form not true, but colloidal solutions in water. In this regard, the physicochemical and biological properties of compounds should be considered in conjunction with data on the size and structure of the particles that the compounds under study form in aqueous solutions. In this work, a comparative study of the dimensional characteristics of aggregates of some amino acid fullerene C_{60} derivatives (AAFDs)† in aqueous solutions was carried out by two methods based on different physical principles: dynamic light scattering (DLS) and small-angle X-ray scattering (SAXS). The DLS method was implemented using two different instruments at scattering angles of 90° and 173°.

The DLS data‡ indicate that the studied AAFDs form polydisperse systems in aqueous solutions. For example, in a solution of *N*-monohydrofullerenyl-L-alanine, four fractions of nanoparticles with different mean hydrodynamic radii were found [Figure S1(*a*),(*b*), see Online Supplementary Materials].

The Zetasizer Nano software allows one to convert the scattered light intensity distribution into a particle volume fraction distribution [Figure S1(*c*)]. The distribution shows what contribution the detected fraction makes to the total volume occupied by the particles in the measured sample. Since the intensity of light

† An aqueous dispersion of fullerene C_{60} was obtained by the known method.[6] *N*-monosubstituted AAFDs have been prepared using α-amino acids such as L- and D-alanine, L- and D-valine, L- and D-aspartic acid, and also using γ-aminobutyric and ε-aminocapronic acids (Acros Organics, purity over 99%) in a one-step synthesis, which consists in the direct addition of an amino acid residue to a fullerene C_{60} molecule according to the previously published method.[7] The concentrations of the obtained aqueous solutions were determined by the gravimetric method.

‡ The hydrodynamic radii of nanoparticles in the studied aqueous solutions of AAFDs were measured by the DLS method using laser radiation with λ = 637.4 nm at a scattering angle of 90° using a Photocor Compact-Z analyzer (Russia). The distributions of hydrodynamic radii were obtained from the measured correlation functions of the scattered light intensity using the DynaLS software (Alango Ltd.) by the cumulant method.[8] Measurements at the reverse scattering angle (173°) were carried out on a Zetasizer Nano ZS analyzer (Malvern Instruments) by measuring fluctuations in the intensity of laser radiation with λ = 633 nm, scattered on nanoparticles of the compounds under study. Sample concentrations were 10^{-4} M.

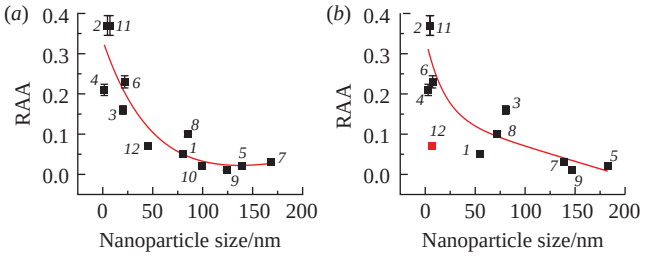

Figure 1 Correlation between RAA values obtained by fluorescent ORAC method and sizes of *N*-monosubstituted AAFD nanoparticles measured on (*a*) Photocor Compact-Z and (*b*) Malvern Zetasizer Nano ZS instruments. Samples tested: (*1*) C_{60}, (*2*) H-C_{60}-L-Ala-OK (synthesis 1), (*3*) H-C_{60}-L-Ala-OK (synthesis 2), (*4*) H-C_{60}-D-Ala-OK (synthesis 1), (*5*) H-C_{60}-D-Ala-OK (synthesis 2), (*6*) H-C_{60}-D-Ala-OK (synthesis 3), (*7*) H-C_{60}-L-Val-OK, (*8*) H-C_{60}-D-Val-OK, (*9*) H-C_{60}-L-Asp-$(OK)_2$, (*10*) H-C_{60}-D-Asp-$(OK)_2$, (*11*) H-C_{60}-γ-GABA-OK and (*12*) H-C_{60}-ε-ACA-OK.

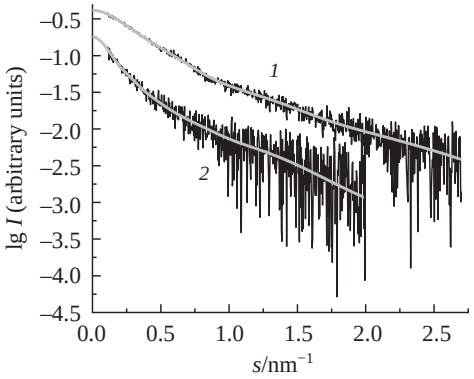

Figure 2 Experimental SAXS intensities (broken lines) and theoretical scattering curves from the found distributions (bold smooth lines) for (*1*) H-C_{60}-L-Ala-OK and (*2*) H-C_{60}-D-Ala-OK nanoparticles.

scattering is proportional to the diameter of the light-reflecting particle multiplied by 10^6, fractions of particles with a smaller average size make a much larger contribution to the total volume occupied by nanoparticles in the solution. Based on this, for further processing and interpretation of the data, we used the radius values for the fractions with the largest volume contribution in the case of the Zetasizer Nano instrument and the radius values for the fractions with the smallest hydrodynamic radius in the case of the Photocor Compact-Z instrument.

The results of DLS studies have shown that in 12 studied AAFD solutions, the hydrodynamic radius of the particles that make the largest volume contribution is in the range from 1.6 to 168 nm (Photocor Compact-Z data) and from 2.9 to 182.7 nm (Zetasizer Nano data). The Pearson pair correlation coefficient between the results obtained using two instruments at different scattering angles is 0.89 (data from one of the samples were excluded as a statistical 'outlier' when calculating the correlation coefficient).

The good convergence of the results is confirmed by the similar nature of the dependence of the relative antiradical activity (RAA) of the compounds, measured in a fluorescent model with thermally initiated generation of free radicals according to the well-known method,[9] on the sizes of nanoparticles, the values of which were obtained using different instruments [Figure 1(*a*),(*b*)]. Briefly, this method consists in observing the drop in fluorescence of 0.01 μM fluorescein under the action of alkyl peroxy radicals formed during the decomposition of the 9.6 mM azo initiator, 2,2′-azobis(2-amidinopropane) dihydrochloride (AAPH), at 37 ± 0.2 °C in the presence or absence of the test sample or reference compound, Trolox. This dependence has the form of a hyperbolic function curve. It should be noted that the ratio of the surface area of a spherical particle to its volume is also related to its radius according to the hyperbolic law, which confirms the determining role of the total surface area of fullerene derivative nanoparticles in their antiradical properties.

In addition to DLS, the dimensional characteristics of H-C_{60}-D-Ala-OK and H-C_{60}-L-Ala-OK nanoparticles in an aqueous colloidal solution were investigated by the SAXS method.[§] Fragments of small-angle scattering intensity curves are shown in Figure 2.

In the case of the L-alanine derivative, fractions of particles with a diameter of 2.2, 4.5 and 8.5 nm and a weak peak at about 17.5 nm were found, while the D-alanine derivative was characterized by fractions of 3.5 and 8.5 nm and a weak peak at about 14 nm [Figure 3(*a*),(*b*)]. Thus, the sizes of nanoparticles obtained by the SAXS method are of the same order of magnitude as the sizes obtained by the DLS method. At the same time, the SAXS method shows that the alanine derivatives form aggregates of a small number of molecules, and the size characteristics of the aggregates present in the solution are related as 1:2:4:8, which indicates that particles consisting of a small number of molecules orderly form larger aggregates like fractal clusters. The results of this work are consistent with the conclusions made earlier by Andrievsky *et al.*[12] about the fractal nature of the formation of aggregates in an aqueous dispersion of fullerene C_{60}, obtained by ultrasonic extraction from toluene, based on the results of electron microscopy. It should be noted that hydrated fullerene C_{60}, as well as its water-soluble derivatives, can structure surrounding water molecules due to the electrostatic interaction between the dipole water molecule and the electrons of π-orbitals of carbon atoms of the fullerene molecule.[13] In this regard, it can be assumed that the values measured by the DLS method will be higher than the actual ones, since the dimensional characteristics are estimated from the Brownian motion not only of the aggregate of molecules of fullerene derivatives, but also of the near-surface layer of water. The SAXS method devoid of this drawback probably shows more reliable results, despite the significant level of noise in the data, the influence of which is leveled by a large number of angular readings and the monotonic nature of the scattering curves.

Concerning the question of changes in the size of nanoparticles, when the concentration of a solution of fullerene C_{60} or its derivatives is changed, different opinions can be found in the scientific literature. For example, Bobylev *et al.*[14] reported that a change in the concentration of a carboxylated derivative of fullerene C_{60} leads to a change in the degree of aggregation, and at lower concentrations, the number of small particles with a diameter of about 5 nm increases. Belavtseva *et al.*[15] noted that when studying the size characteristics of aggregates of *N*-monosubstituted AAFDs by the diffusion method, in some of the studied compounds, a change in the size of associates was observed when the solution concentration changed; however, for some objects, changes in concentration in the range

[§] SAXS intensities from solutions were measured on an AMUR-K small-angle X-ray diffractometer (FSRC 'Crystallography and Photonics', Moscow, Russia) with an OD3-M linear position-sensitive detector at a wavelength of 0.1542 nm (CuKα line, pyrolytic graphite monochromator) and a Kratky collimation system. The X-ray beam cross section was 0.2 × 8 mm, and the angle range was $0.14° < 2\theta < 15.8°$. The sample was placed in a quartz capillary with a diameter of 1.0 mm. The measurement time was 2 h. The experimental data were normalized to the intensity of the incident beam, then the scattering on the capillary with water was subtracted, and a correction for collimation distortions was introduced.[10]

Based on the scattering data, the volume size distributions of nanoparticles in solutions were calculated using the VOLDIS program according to the published method,[11] assuming a spherical shape of the nanoparticles. This assumption is not exact, but, as practice shows, it gives adequate estimates of the effective average sizes of scattering inhomogeneities with an accuracy of no worse than 10–30% even in the case of anisometric shapes.

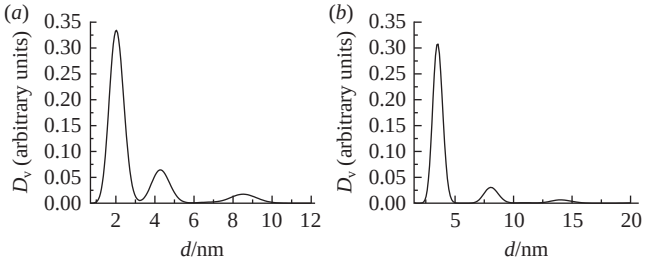

Figure 3 Volume distributions of particle diameters *d* calculated from SAXS data in the approximation of spherical shape of (*a*) H-C_{60}-L-Ala-OK and (*b*) H-C_{60}-D-Ala-OK nanoparticles.

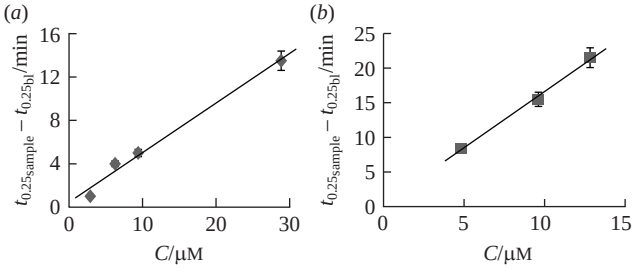

Figure 4 Dependence of the increase in the conversion time of 25% of the initial oxidized compound relative to the control experiment ($t_{0.25_{sample}} - t_{0.25_{bl}}$) on the concentration of H-C_{60}-D-Ala-OK in the reaction medium during the oxidation of (*a*) fluorescein and (*b*) phosphatidylcholine liposomes.

from 75 to 150 mg dm^{-3} did not lead to changes in the diffusion coefficient and, consequently, in the size of associates. In this work, we found that changing the concentration of *N*-monohydrofullerenyl-L-alanine solution from 10^{-3} to 10^{-5} M does not lead to a change in the nanoparticle radius determined by DLS (Table 1). The concentration of the test sample was varied by diluting it with deionized water with a resistivity of 18.2 MΩ cm.

The invariance of the size of *N*-monosubstituted AAFD nanoparticles upon dilution of the solution is indicated by the linear character of the dependence of the inhibitory activity with respect to the AAPH-induced oxidation of fluorescein and phosphatidylcholine (the results for phosphatidylcholine were obtained according to the well-known method[16]) on the concentration of the fullerene derivative in the range from 10^{-7} to 10^{-6} M [Figure 4(*a*),(*b*)]. Briefly, this method consists in the spectrophotometric observation of the accumulation of diene conjugates at an absorption maximum of 234 nm upon oxidation of 0.1 mg cm^{-3} of phosphatidylcholine liposomes by alkyl peroxide radicals formed during the thermal decomposition of 0.33 mM AAPH at 37 ± 0.2 °C in the presence of 5–13 μM of the test sample.

The experiments have shown that *N*-substituted amino acid derivatives of fullerene C_{60} in aqueous solutions form aggregates characterized by a polydisperse size distribution. The data obtained by the DLS method at different scattering angles correlate well with each other. At the same time, the SAXS data indicate that the studied compounds form nanoparticles from a small number of molecules, which can orderly aggregate to form fractions of larger particles, the sizes of which are related by the ratio 1 : 2 : 4 : 8. The hyperbolic dependence of the antiradical activity on the nanoparticle size indicates that the main role in the observed antiradical properties is played by the active surface area of the particles. The study of the size–concentration dependence by the DLS method, as well as the linear concentration dependence of the antiradical activity in model systems, indicates that the degree of aggregation of AAFDs in aqueous solutions does not change upon dilution. The results of this study provide new information on the behavior of water-soluble AAFDs in aqueous solutions and may be of interest to researchers in the field of fullerene chemistry.

Table 1 Dependence of the size of H-C_{60}-L-Ala-OK aggregates (DLS, scattering angle 173°) on solution concentration.

Concentration of H-C_{60}-L-Ala-OK/M	Radius of nanoparticles/nm
1×10^{-3}	4.2 ± 2.7
1×10^{-4}	4.5 ± 0.8
1×10^{-5}	4.8 ± 1.1

This work was supported by the Ministry of Science and Higher Education of the Russian Federation. Studies by small-angle X-ray scattering were carried out within the framework of the state assignment of the Federal Research Center 'Crystallography and Photonics' of the Russian Academy of Sciences.

Online Supplementary Materials

Supplementary data associated with this article can be found in the online version at doi: 10.1016/j.mencom.2023.10.028.

References

1 A. G. Bobylev, O. A. Kraevaya, L. G. Bobyleva, E. A. Khakina, R. S. Fadeev, A. V. Zhilenkov, D. V. Mishchenko, N. V. Penkov, I. Y. Teplov, E. I. Yakupova, I. M. Vikhlyantsev and P. A. Troshin, *Colloids Surf., B*, 2019, **183**, 110426.
2 M. Azizi-Lalabadi, H. Hashemi, J. Feng and S. M. Jafari, *Adv. Colloid Interface Sci.*, 2020, **284**, 102250.
3 M. Gaur, C. Misra, A. B. Yadav, S. Swaroop, F. Ó. Maolmhuaidh, M. Bechelany and A. Barhoum, *Materials*, 2021, **14**, 5978.
4 V. S. Romanova, N. Yu. Shepeta, Z. S. Klemenkova and K. A. Kochetkov, *Mendeleev Commun.*, 2021, **31**, 844.
5 V. A. Brotsman, N. S. Lukonina and A. A. Goryunkov, *Russ. Chem. Bull.*, 2023, **72**, 20.
6 G. V. Andrievsky, M. V. Kosevich, O. M. Vovk, V. S. Shelkovsky and L. A. Vashchenko, *J. Chem. Soc., Chem. Commun.*, 1995, 1281.
7 V. S. Romanova, V. A. Tsyryapkin, Yu. I. Lyakhovetsky, Z. N. Parnes and M. E. Vol'pin, *Russ. Chem. Bull.*, 1994, **43**, 1090 (*Izv. Akad. Nauk, Ser. Khim.*, 1994, 1154).
8 P. Stepanek, in *Dynamic Light Scattering: The Method and Some Applications*, ed. W. Brown, Clarendon Press, Oxford, 1993, pp. 177–241.
9 V. A. Volkov, M. V. Voronkov, N. N. Sazhina, D. V. Kurilov, D. V. Vokhmyanina, O. V. Yamskova, Yu. Ts. Martirosyan, D. L. Atroshenko, L. Yu. Martirosyan and V. S. Romanova, *Kinet. Catal.*, 2021, **62**, 395 (*Kinet. Katal.*, 2021, **62**, 343).
10 L. A. Feigin and D. I. Svergun, *Structure Analysis by Small-Angle X-Ray and Neutron Scattering*, ed. G. W. Taylor, Springer, New York, 1987.
11 V. V. Volkov, *Crystals*, 2022, **12**, 1659.
12 G. V. Andrievsky, V. K. Klochkov, E. L. Karyakina and N. O. Mchedlov-Petrossyan, *Chem. Phys. Lett.*, 1999, **300**, 392.
13 G. Andrievsky, V. Klochkov and L. Derevyanchenko, *Fullerenes, Nanotubes Carbon Nanostruct.*, 2005, **13**, 363.
14 A. G. Bobylev, N. V. Penkov, P. A. Troshin and S. V. Gudkov, *Biophysics*, 2015, **60**, 30 (*Biofizika*, 2015, **60**, 38).
15 E. M. Belavtseva, E. Y. Kichenko, V. S. Romanova, Z. N. Parnes and M. E. Vol'pin, *Russ. Chem. Bull.*, 1996, **45**, 831 (*Izv. Akad. Nauk, Ser. Khim.*, 1996, 876).
16 N. N. Sazhina, I. G. Plashchina, M. G. Semenova and N. P. Pal'mina, *Colloid J.*, 2020, **82**, 69 (*Kolloidn. Zh.*, 2020, **82**, 89).

Received: 8th June 2023; Com. 23/7188